JOURNAL OF MATERIALS SCIENCE 33 (1998) 1385–1388

# Creation of TiN paths on titanium alloy OT4-1 by the use of a laser beam

J. ZIMNICKI, K. ROŻNIAKOWSKI
*Institute of Physics, Technical University of Lodz, ul. Wolczanska 219, 93-005 Lodz, Poland*

B. WENDLER
*Institute of Materials Engineering, Technical University of Lodz, ul. Stefanowskiego 1, 90-924 Lodz, Poland*

W. KALITA, J. HOFFMAN
*Institute of Fundamental Technological Research, ul. Swietokrzyska 21, 00-049 Warszawa, Poland*

TiN paths have been created on the surface of the titanium alloy OT4-1 by the use of a laser beam. The results of investigations of structure, phase composition, microhardness and surface roughness of the created TiN paths are given in the paper. The paths created in the work are inhomogenous two-phase mixtures of TiN and α-Ti, in which the TiN phase with strong (2 0 0) texture is predominant over the other phase and presents a dendritic structure.


## 1. Introduction

Different methods and techniques [1] are available for modification of metal surface and, in particular, to create titanium carbides or nitrides on its surface [2, 3]. Laser modification of the surface of bulk titanium samples in an appropriate atmosphere presents another possibility. Recently many papers have been devoted to TiN creation by the use of $CO_2$ lasers [4–6]. The method is characteristic in that the time necessary for TiN creation is relatively short and, moreover, that the surface modification is well localized and accompanied by a liquid phase which precludes distortions of the laser-treated samples. Additionally, the created layers are considerably thicker than those obtained by the use of many other methods.

The principal objective of the work was to create single or multiple TiN paths on the surface of the OT4-1 titanium alloy by the use of $CO_2$ laser radiation operating in nitrogen atmosphere at normal pressure.

## 2. Experimental procedure

Samples 4 mm thick were cut from a sheet of titanium grade OT4-1 (alloyed with approximately 1.5 wt% Al and 1.3 wt% Mn). The samples were mounted onto a plane stage so that the flat specimen surface (of roughness parameter, $R_a = 0.79\,\mu m$) was normal to incident $CO_2$ laser radiation used for local heating of the sample. The laser was working in continuous mode at the wavelength, $\lambda = 10.6\,\mu m$, 1 kW power, beam diameter 0.36 mm and beam defocusing, $\Delta f \approx 2.5$ mm. The stage was heated with the specimen moving uniformly in a plane perpendicular to incident radiation so that the laser beam was moving along straight lines on the specimen surface. The laser beam moved with three different velocities $v_1 = 0.042\,m\,s^{-1}$, $v_2 = 0.066\,m\,s^{-1}$ and $v_3 = 0.10\,m\,s^{-1}$. If one takes into account that the exposure time $\tau = v/d$, where $v$ and $d$ denote the linear velocity of the laser beam and its diameter, respectively, the effective times of heating for the three velocities are equal to $8.5 \times 10^{-3}$ s, $5.4 \times 10^{-3}$ s, and $3.6 \times 10^{-3}$ s, respectively, and the estimated power density $Q \approx 10^{10}\,W\,m^{-2}$. When operating with the laser beam, a nitrogen flow through a nozzle collinear to the beam was employed and the linear velocity of the gas flow at the outlet of the nozzle was $20\,m\,s^{-1}$. To obtain broad bands, multiple parallel paths were created so that the overlap of any two adjacent paths was equal to 30%. The morphology and structure of those bands were examined by optical microscopy, scanning electron microscopy (SEM) (Tesla 300) and X-ray analysis (Siemens powder diffractometer D-500). Independently the Vickers microhardness and the surface roughness of the bands have been measured using a Zwick 3212 hardness tester with a diamond pyramid at a load of 0.5 N (for microhardness) and using a Hommel tester T 1500G profilometer (for the roughness parameter, $R_a$).

## 3. Results and discussion

### 3.1. Morphology

The colour of the surface of single paths as well as of the broad bands was yellow (typical for a TiN phase) and presented a characteristic rippled structure. At the same time the roughness parameter, $R_a$, of the surface

increased to 0.90 μm. In the broad bands, numerous lateral cracks linking adjacent paths were observed (generally in the direction normal to the paths). The width of those cracks was approximately 5 μm and their frequency was about two cracks per millimetre. Other cracks, narrower than the former cracks, were oriented parallel to the paths and linked wide lateral cracks (Fig. 1). The density of the cracks did not depend on the velocity of linear motion of the specimen. In [4, 5] it was suggested that the cracks are due to excess nitrogen in the molten metal. The constant density of cracks in the present work can be explained if one takes into account that the nitrogen flow rate was always the same in the experiment.

## 3.2. Structure

Some examples of diffractograms characteristic for the broad bands are given in Fig. 2. One can see that at least two phases are present: α-Ti and δ-TiN (with a predominant amount of that latter). The grains of the δ-TiN phase demonstrate a strong (2 0 0) texture, the diffraction peaks being broader and the parameter, *a*, of the elementary cell smaller than those of standard TiN phase (according to [9]). Those differences can be explained if one takes into account that at least some of the positions of nitrogen atoms in the elementary cells can be occupied by oxygen [10] which decreases cell dimensions; broadening of the peaks can be due to local differences of the chemical composition in the molten zone as well as to the appearance of microstresses when rapidly cooling a multiphase alloy. Insertion of oxygen atoms into elementary cells should be linked to their penetration from the surrounding atmosphere when using a nitrogen flow, as well as from a thin $TiO_2$ layer on the surface of untreated primary titanium sheet used for the samples. The other phase which remains in the molten zone, α-Ti, demonstrate rather (1 0 1) texture; however, in that case the (1 0 1) peak is shifted to smaller diffraction angle in comparison with that of the standard (Fig. 2). That displacement could be due to interstitial nitrogen (or eventually oxygen) atoms as well as to compressive stresses tangent to the path's surface and normal to its axis. Another phase, $Ti_2N$, which could be taken into consideration from the Ti–N equilibrium diagram was not observed (if one neglects the small peak in the vicinity of $2\theta \approx 46^\circ$ in Fig. 2 which coincides with the position of the (1 0 1) peak of that phase). The absence of the $Ti_2N$ phase can be explained if one takes into account that the structure obtained in the cooling of the molten zone is far from equilibrium, the cooling rate estimated for the conditions given in Section 2 is of the order $10^5$–$10^6$ K $s^{-1}$ which is too high for the $Ti_2N$ phase to be formed when cooling the molten zone [6]. One should bear in mind, however, that the penetration depth (into a bulk titanium sample) of the X-ray Co Kα radiation used in the experiment for the diffraction angle 2θ in the range 40–60° does not exceed 10 μm, which is much less than the total thickness of the molten zone (see Section 3.3).

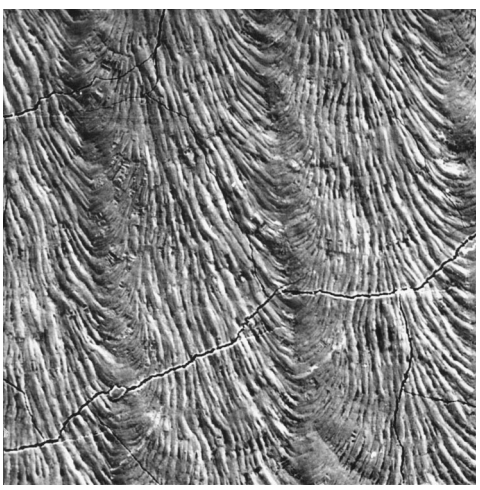

*Figure 1* Lateral cracks on the surface of TiN paths. (Magnification, 200×.)

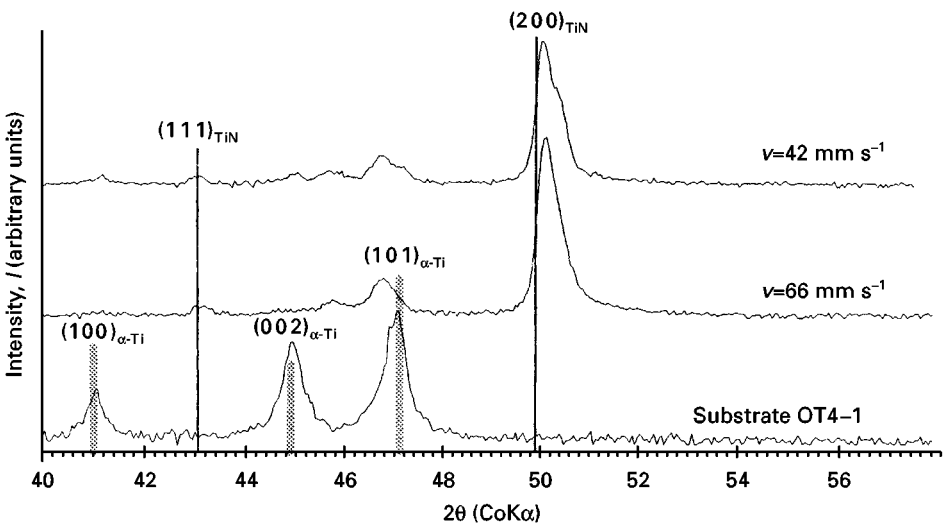


*Figure 2* Diffraction patterns for two different TiN bands in comparison with that for the untreated surface of the OT4-1 alloy. ▨ α-Ti [7]; |, TiN Oshornit [8].

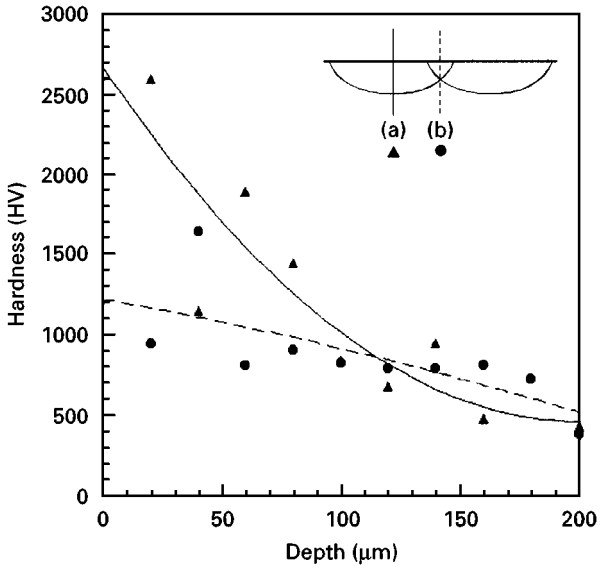


*Figure 3* Vickers microhardness of the laser beam-treated material at different depths from the surface: (a) in the central region of a treated path; (b) in the zone of overlap of adjacent paths.

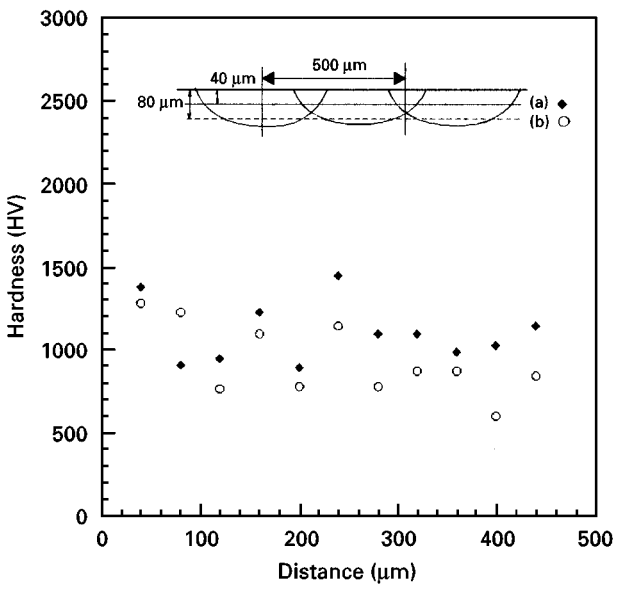


*Figure 4* Variations in Vickers microhardness in the direction parallel to the surface at two different depths, 40 and 80 μm, from the surface.

## 3.3. Microhardness

The results of microhardness measurements on polished sections perpendicular to the paths' axes are given in Figs 3 and 4. In Fig. 3 the microhardness at different depths is presented (one curve for the central region of the path and the other for the zone of overlap of adjacent paths). In Fig. 4 the results of the measurements in the direction parallel to the path's surface are given at two different depths, 40 and 80 μm. The highest measured values of the vickers microhardness was 2600 HV 0.05, which corresponded to that for the stoichiometric TiN phase [11], the other values being much less, from 1600 HV 0.05 down to the lowest value of 400 HV 0.05. The latter low microhardness (which was also measured near the path's surface) could be due to too low as nitrogen concentration in the TiN phase as well as to other phases (such as α-Ti) present in the region under consideration. The great variability of the microhardness measurements can also be linked to local chemical changes and to local changes in phase composition of the molten zone. According to the conditions given in Section 2, the density of the power delivered to the path's surface was less than that necessary to boil titanium; in that case the mixing in the molten zone arises mostly because of temperature gradients of the surface tension coefficient.

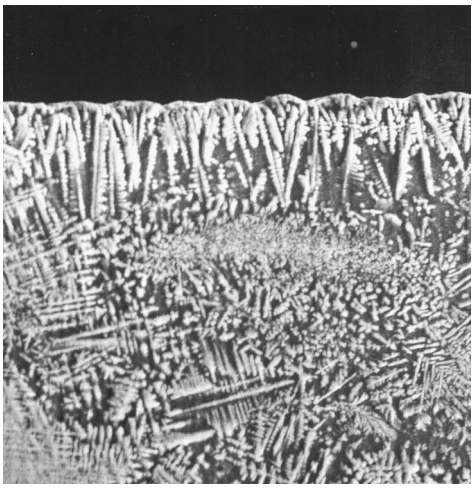

*Figure 5* Scanning electron micrograph of a polished section normal to the direction of the path. The section was etched in with a 1:1:3 solution of a hydrofluoric and nitric acids in glycerine. Dendrites in the vicinity of the path's surface can be seen. (Magnification, 1200×.)

## 3.4. Metallurgy

SEM examinations demonstrate that dendrites are present in the molten zone. The dendrites which are present in the region near to the path's surface have axes perpendicular to it (Fig. 5), whereas the axes of dendrites which are present far inside the molten zone are randomly distributed. That latter proves that there is a mixing in the zone molten by the laser beam (probably due to convection as a result of surface tension forces).

## 3.5. Numerical estimations

The results of the experiments prove that melting of the thin layer of titanium alloy OT4-1 during laser beam irradiation in a nitrogen atmosphere is accompanied by penetration of nitrogen atoms interstitially into α-Ti phase as well as by chemical reactions producing the δ-TiN phase; these compose a two-phase material very different from the initial alloy. In further discussion it will be shown that the parameters of the molten zone in the experiment are near to those deduced from a particular model of laser beam interaction with metallic specimen.

The power of the electromagnetic radiation absorbed by metallic target depends essentially on the chemical composition and roughness of the substrate.

The absorbtion "depth", $l$, in a metal such as titanium is approximately $1 \times 10^{-7}$–$1 \times 10^{-8}$ m [12]; therefore one can say that in the experiments performed in the work the condition $d \gg 1$, where $d$ denotes the laser beam diameter, was fulfilled.

On the other hand it is well known that determination of the temperature distribution in a sample subjected to laser irradiation by means of solution of the thermal conductivity equation is a very complicated task and the solution has a numerical form. However, assuming that the thermal coefficients do not depend on the temperature, the solution is relatively simple if one makes use of the Green function method [12]. One can obtain an even simpler expression for the temperature distribution on making some qualitative assumptions and estimating only the thickness, $h$, of the molten zone by use of the formula given in [3] :

$$h \approx 2(a\tau)^{1/2} \ln\left(\frac{2\alpha Q\sqrt{(a\tau)}^{1/2}}{KT_t}\right) \quad (1)$$

where $a = K/\rho c$ denotes thermal diffusivity of the material under consideration, $K$ its thermal conductivity, $\rho$ the density, $c$ the specific heat, $\alpha$ the effective absorbtion coefficient and $T_t$ the melting point of the material. The effective absorption coefficient, $\alpha$, in Equation 1 can be estimated by making use of the highest linear velocity of the liquid–solid interface [14]:

$$v_m = \alpha Q(\lambda + \rho c T_t)^{-1} \quad (2)$$

where $\lambda$ is the heat of fusion of the material.

The highest linear velocity of the liquid–solid interface was estimated on the assumption that the time of its displacement is approximately equal to the heating time, $\tau$ (which is quite reasonable if one takes into account that at the rather high power density used in the experiment the time necessary for the surface temperature to change from the ambient temperature to the melting temperature is negligible in comparison with the total heating time, $\tau$). Having measured the mean experimental values of the melting depths (210, 178 and 152 μm) for three different heating times $\tau$, the corresponding velocities were $v_m^1 = 0.024\ \mathrm{m\,s^{-1}}$, $v_m^2 = 0.033\ \mathrm{m\,s^{-1}}$ and $v_m^3 = 0.043\ \mathrm{m\,s^{-1}}$ and could be used in Equation 2 to estimate the absorbtion coefficient, $\alpha$. Making use of the obtained $\alpha$ values as well as of the other values known for the alloy OT4-1 ($\lambda = 1.5 \times 109\ \mathrm{J\,m^{-3}}$, $T_t = 1940$ K, $\rho \approx 4500\ \mathrm{kg\,m^{-3}}$, $c = 841\ \mathrm{J\,Kg^{-1}\,K^{-1}}$ and $K = 16.3\ \mathrm{W\,m^{-1}\,K^{-1}}$ [15, 16]) the following melting depths were calculated: $h_1 =$ 236 μm, $h_2 = 213$ μm and $h_3 = 182$ μm, which correspond well to the real values of the penetration depths for different laser beam velocities.

## 4. Conclusions

1. Continuous-mode $CO_2$ laser beam surface melting of titanium alloys in a nitrogen atmosphere at normal pressure seems to be an effective method for the creation of hard, narrow or broad bands or single paths on the surface of those alloys.

2. The surface of the created paths or bands has a characteristic rippled morphology and different (lateral and longitudinal) cracks are present in it; the thickness of the molten zones in the paths is dependent on the linear velocity of movement of the laser beam.

3. Two phases have been identified in the surface region of the paths by means of X-ray analysis: α-Ti and δ-TiN, the volume fraction of the latter being predominant and the majority of (2 0 0) planes in its crystallites being parallel to the paths' surfaces. This statement does not preclude the fact that other phases, e.g., $Ti_2N$ or titanium oxides, could also be present in that surface region but in rather a low volume fraction, or even in a greater volume fraction but at greater depth.

4. The Vickers microhardness of the paths changes in the range from approximately 2600 HV 0.05 on the path's surface down to about 400 HV 0.05 deep inside the molten region.

5. The melting depths estimated from numerical calculations in the frameworks of a simple theory by Vedenov and Gladusch [13] correspond well to those obtained from direct measurements.

## References


1. T. BURAKOWSKI and T. WIERZCHON, in "Inzynieria powierzchni metali" edited by E. Czarzasta, (WNT, Warsaw, 1995) p. 237 (in Polish).
2. W. LENGAUER, in Proceedings of the Conference on Trends and New Applications in Thin Films, Dresden, March 1994, edited by G. Hecht, F. Richter and J. Hahn (Deutsche Gesellschaft für Metallkunde Informationsgesellschaft, Darmstudt, 1994) p. 614.
3. B. WENDLER, *Mater. Sci. Engng* **A163** (1993) 215.
4. S. MRIDHA and T. N. BAKER, *Processing of Adv. Mater.* **4** (1994) 85.
5. S. MRIDHA and T. N. BAKER, *Mater. Sci. Engng* **A188** (1994) 229.
6. L. JIANGLONG, L. QIQUAN and Z. ZHIRONG, *Surf. Coatings Technol.* **57** (1993) 191.
7. Joint Committee on Powder Diffraction Standards, "Powder diffraction file" (International Center for Diffraction Data, Swathmore, PA, 1954) Card 5–682.
8. Joint Committee on Powder Diffraction Standards, "Powder diffraction file" (International Center for Diffraction Data, Swathmore, PA, 1987) Card 38–120.
9. Joint Committee on Powder Diffraction Standards, "Powder diffraction file" (International Center for Diffraction Data, Swathmore, PA, 1953) Card 6–642.
10. E. K. MOLTCHANOVA, in "Atlas diagramm sostoiania titanovykh splavov" edited by S. G. Glazunova (Mashinostroenie, Moscow, 1964) p. 376 (in Russian).
11. H. J. GOLDSCHMIDT, in "Interstitial alloys" (Butterworth, London, 1967) p. 302.
12. H. S. CARSLOW and J. C. JAEGER, in "Conduction of heat in solids" 2nd edn (Clarendon, Oxford, 1959) pp. 50, 487.
13. A. A. VEDENOV and G. G. GLADUSCH, in "Fizicheskie processy pri lasernoi obrabotkie materialov" edited by O. P. Dunaeva (Energoatomizdat, Moscow, 1995) p. 29 (in Russian).
14. W. W. DULEY, in "Laser processing and analysis of materials" (Plenum, New York, 1993) p. 113.
15. R. DOMANSKI, in "Promieniowanie laserowe-oddzialywania na ciala stale" edited by A. Zolcinska (WNT, Warsaw, 1990) p. 270 (in Polish).
16. L. N. PARIKOV and Yu. S. YURCHENKO, in "Teplovyie svoistva metallov i splavov" edited by L. N. Parikov (Naukova Dumka, Kiev, 1985) pp. 178, 220, 344 (in Russian).



*Received 6 February 1996*
*and accepted 24 September 1997*